Marine Pollution Bulletin 209 (2024) 117110

Contents lists available at ScienceDirect

Marine Pollution Bulletin

journal homepage: www.elsevier.com/locate/marpolbul

A regional Lagrangian model to evaluate the dispersion of floating macroplastics in the North Atlantic Ocean from land and river sources in the western coast of Spain

Sara Cloux [a,b,*], Patricia Pérez [c], Hilda de Pablo [d,e], Vicente Pérez-Muñuzuri [a]

[a] CRETUS Research Center, Nonlinear Physics Group, Faculty of Physics, University of Santiago de Compostela, Spain
[b] IFISC (CSIC-UIB), Instituto de Física Interdisciplinar y Sistemas Complejos, Campus Universitat de les Illes Balears, E-07122, Palma de Mallorca, Spain
[c] Centro Oceanográfico de Vigo, Instituto Español de Oceanografía (IEO), CSIC, Vigo, Spain
[d] MARETEC, Instituto Superior Tecnico, Universidade de Lisboa, Portugal
[e] Faculty of Engineering, Lusófona University, Campo Grande, Lisbon, Portugal

ARTICLE INFO

Keywords:
Macroplastics
Lagrangian-tracking model
Marine litter hotspots
Transboundary pollution
North Atlantic
Spain

ABSTRACT

Marine plastic litter is an emerging global problem with serious environmental and economic consequences. Once deposited in the ocean, it is transported by currents for long periods of time, making it a transboundary problem. The variety of plastic items makes the study of their transport in the ocean system a challenge. Identifying the sources and analyzing the extent of their dispersion/accumulation can help solve the problem on a global scale. In this study, using modeling tools, the dispersion of particles from land-based sources located on the Spanish Atlantic coast was analyzed over a seven-year period. The results show that the highest concentrations of plastic are found near the coast. The particle dispersion is consistent with the oceanic dynamics of each region studied. The seasonal behavior of plastics arriving in neighboring countries was also analyzed. The time-varying patterns are consistent with local hydrodynamics and the general circulation of the ocean.

1. Introduction

One of the biggest environmental pollution problems that affects the entire world is plastic marine litter (Amelia et al., 2021; Krause et al., 2020; Rangel-Buitrago et al., 2020). Poor management of this waste on land and in maritime activities usually means that it ends up reaching the sea, beginning a long period of degradation as it is carried by ocean currents. Because they can spend many years floating or submerged in the ocean, many of these plastics break down into small fragments through various agents such as wind, salinity, solar radiation, biofouling, temperature and mechanical stress due to currents and wave motion (Min et al., 2020; Wayman and Niemann, 2021). It is important to differentiate between macroplastics ($\geq$ 5 mm) and microplastics ($\leq$ 5 mm). Numerous well-known species have already been harmed by their entry into the food chain, both physically and as toxicants due to the chemical pollutants they may contain (Herrera et al., 2022; Bhagat et al., 2020; Hwang et al., 2020).

Although the amount, distribution, and origin of plastic debris on beaches and in deep seas are virtually unknown (Onink et al., 2021), it is generally accepted that this type of pollutant causes negative impacts on marine and coastal ecosystems, fisheries, and tourism (Alfaro-Núñez et al., 2021; Williams and Rangel-Buitrago, 2019; Karbalaei et al., 2018). Estimates based on observations suggest that only a small percentage (less than 300 K tons, $\approx$ 2% of plastics entering the ocean per year) of the discarded plastics remain on or near the surface of the open ocean, despite the fact that the majority of plastics produced have a lower density than seawater and should be found floating in the ocean or washing up on shore. From estimates of floating marine plastic stock, macrolitter is considered to represent a large portion of the plastic mass entering the ocean (Eriksen et al., 2014). Thus, a precise estimation of the speed with which plastic leaves the ocean surface through a variety of processes, such as degradation, biological ingestion, settling, and beaching, as well as the rate of transit from one place to another, is required to respond to this topic (Sutherland et al., 2023).

However, the exact plastic emission locations and associated emission rates are not well known. Both visual studies of plastic-emitting areas and remote sensing, together with the use of statistical methods, allow a first approximation of the amount of plastics entering the ocean

* Corresponding author at: CRETUS Research Center, Nonlinear Physics Group, Faculty of Physics, University of Santiago de Compostela, Spain.
E-mail address: saracloux@gmail.com (S. Cloux).

https://doi.org/10.1016/j.marpolbul.2024.117110
Received 8 February 2024; Received in revised form 24 September 2024; Accepted 4 October 2024
Available online 17 October 2024

(Lavender, 2022; Liu et al., 2020; van Calcar and van Emmerik, 2019; Van Emmerik et al., 2018). In the case of rivers, the amount of plastics emitted can be related to the size of the river basin and the population that inhabits that area (González-Fernández et al., 2021). As these emission rates depend on many other factors, such as river flooding, estuary residence time, or eventual areas of retention (de Pablo et al., 2022), it is often difficult to determine an exact amount. Bauer-Civiello et al. (2019) also studied the influence of stormwater systems as a rarely identified input for plastics in rivers. Other land emissions should be considered, such as coastal population centers, ports, and bathing areas (Jambeck et al., 2015; Masiá et al., 2021). Marine sources are also important contributors due to the high number of items related to maritime activities that are found drifting in the open sea or stranded on the coast. Special concern is raised by nets and other fishing gears in which animals such as seabirds, turtles, cetaceans, or fish can be trapped (Ryan, 2018; Duncan et al., 2017; Tulloch et al., 2020). Once emission points are established, computational circulation models can be used to understand the movement described by these items once they are released into the sea (Van Sebille et al., 2020; Iskandar et al., 2021).

Transport of plastics can be modeled as passive Lagrangian tracers that because of their (positive or negative) buoyancy, they can (slowly) rise or settle through the fluid due to the hydrodynamics, Stokes drift, and/or wind (Carlson et al., 2017; Chassignet et al., 2021; Politikos et al., 2020; Turrell, 2020; Khoirunnisa et al., 2020; Sousa et al., 2021; Jalón-Rojas et al., 2019a). However, larger (or inertial) particles, with a larger Stokes number, move differently from the surrounding fluid (Maxey and Riley, 1983), and other forces beyond their slow vertical motion due to buoyancy, as drag forces, Basset history force that captures the lagging boundary layer development with changing relative velocity, added mass, and lift forces should be included into the model. Summarizing, for a correct modeling of macroplastic transport, the inertial effects, mechanical effects (degradation, biofouling, beaching, etc) and the amount, type, and sizes of the plastics entering the ocean should be taken into account. To our knowledge, this type of study has not been done so far.

Lagrangian models track virtual particles in a simulated fluid flow, driven by advection from surface ocean currents and diffusion. For example, Stuparu et al. (2015) used the Delft3D model to simulate water flow and sediment transport in the North Sea at the local scale, specifically using the PART module for particle tracking. Sousa et al. (2021) applied the Delft3D model to investigate transport mechanisms within the intricate channel system of the Rotterdam harbor and the Vigo estuary, respectively. In another study, Carlson et al. (2017) performed a particle tracking analysis in the Adriatic Sea using the Particle Tracking and Analysis Toolbox (PaTATO) for Matlab, comparing simulation results with field data. The study by Turrell (2020) employed a simplified particle tracking model with an idealized shoreline to explore the interaction between variable winds and water levels (VaWWL) along a shoreline. OceanParcels model (Lange and van Sebille, 2017) is a Lagrangian tool that allows tracking individual particle trajectories under the influence of physical and biogeochemical processes. It is highly flexible and interoperable with other oceanographic models and datasets, facilitating the inclusion of a variety of particles and behaviors. OpenDrift (Dagestad et al., 2018) is a highly configurable Lagrangian model and can be integrated with various oceanic and atmospheric circulation models, allowing the simulation of processes such as advection, diffusion and vertical mixing. It is applicable in multiple areas, from pollutant dispersion to the transport of marine organisms and ice. Jalón-Rojas et al. (2019b) performed a sensitivity analysis of the TrackMPD model parameters to show the strong influence of different processes on the transport and fate of marine plastics, highlighting the importance of the three-dimensional approach. Sinking has a significant impact on the trajectory and fate of plastics, followed by turbulent dispersion and re-entry into the sea. The density, size and shape of the particles determine their buoyancy and vertical movement, being especially relevant in shallow waters.

These models can also be effectively used as sensitivity analysis tools to study the influence of different parameters. For example, Critchell and Lambrechts (2016) used the SLIM 2D model, explored the effects of resuspension, degradation, diffusivity, wind action and emission points on plastic dispersion, highlighting the need to consider the impacts of wind, waves and complex topography on beach deposition. Similarly, Tsiaras et al. (2021) conducted an 8-year simulation to identify patterns of micro- and macroplastic accumulation in various ocean layers and beaches, linking these distributions to sewage sources near metropolitan areas and noting the significant impact of biofouling-induced subsidence on microplastic concentrations. Their study revealed that larger microplastics accumulated in convergence zones with anticyclonic circulation, while macroplastics were influenced by wind drag.

The Bay of Biscay (Pereiro et al., 2018, 2019; Declerck et al., 2019; Basurko et al., 2022; Ruiz et al., 2022), Galician Rías (NW Spain) (Sousa et al., 2021; Cloux et al., 2022), Gulf of Cadiz (Mecho et al., 2020) and Canary islands (Cividanes et al., 2024; Hernández-Sánchez et al., 2021; Baztan et al., 2014) have been highlighted by recent research for floating plastics, based on Lagrangian calculations using numerical models and observations. The potential accumulation zones and the contributions of different emission sources have been calculated and compared to previous studies. In this paper, the dispersion of floating macroplastics that enter into the ocean from rivers and on-land sites on the Atlantic Spanish coast is analyzed.

We used the MOHID-Lagrangian tool (www.mohid.com) that has been recently validated by Cloux et al. (2022) in a regional domain. This novel model can estimate the trajectories for a large number of particles (up to one million) considering different phenomena such as hydrodynamics, waves, and windage. The macroplastics are assumed as passive tracers with a density smaller than water and small Stokes number. The strength of this model, compared to others cited above, lies in its advanced beaching parameterization capabilities and its high computational capacity to track a large number of particles. The code is written specifically for multi-threaded and shared memory computers. It allows users to set a specific depth threshold at which particles are considered stranded in the sand and to define the probability of stranding events. These parameters enable the modeling of diverse accumulation scenarios. Furthermore, the model is robust enough to distinguish between coastal accumulations from different emission sources, facilitating separate evaluations of each source's impact. Here we present a study considering two emission sources, rivers and land, and three emission regions (northern Spain, Gulf of Cadiz and Canary Islands) on the Spanish coasts. Since the contribution from rivers is expected to depend on river flows, a time-varying emission rate has been considered. For land-based sources, a continuous emission has been established, weighting the relative importance between sources according to the values provided by MAPAMA (Ministerio de Agricultura y Pesca and Públicas) (2012a,b). A 7-year simulation was performed for each source separately. It has been assumed that neutral floating litter behaves like Lagrangian tracers that are only transported by surface currents. The transboundary pollution in the western coasts of France, Portugal and Morocco will be also studied.

2. Study area

This paper focuses on the dispersion of particles originating from three regions of the Spanish Atlantic coast; Cantabrian sea, the Gulf of Cadiz and the Canary Islands, through the North Atlantic Ocean and the Mediterranean Sea. The surface circulation of each of these areas and its temporal variability are briefly described below.

The circulation of the North Atlantic Ocean (Fig. 1(a)) is well described in the literature. The North Atlantic circulation can be described as starting in the Gulf Stream (Krauss, 1986; Dietrich and Kalle, 1957), where water masses flow parallel to the east coast of North America until they reach Cape Hatteras. According to Talley (2011) and Mann (1967, 1972), the Gulf Stream bifurcates near the Newfoundland

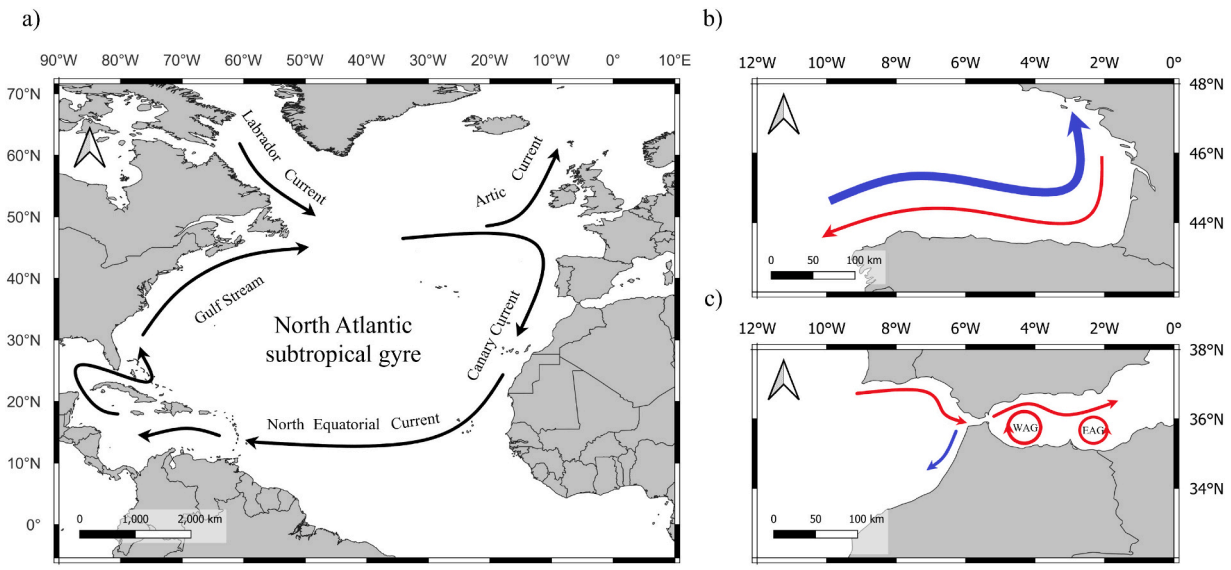

Fig. 1. Surface currents in the study area. General circulation in the Atlantic Ocean (a), and the seasonal behavior of the currents in the Bay of Biscay (b) and in the South of Spain (c). Red arrows denote the dynamics for the warmer seasons, while the blue arrows correspond to the dynamics for the colder months. (For interpretation of the references to colour in this figure legend, the reader is referred to the web version of this article.)

Banks into two branches. One of the branches continues eastward at an altitude of 52°N and forms the North Atlantic Current. Mann (1972) identified the area around 42°N and 42°W as the center of a permanent anticyclonic gyre. Once the current reaches the west coast of Europe, it splits into two branches, one in a northerly direction that becomes the Arctic Current and the other in a southerly direction that becomes the Canary Current, the Atlantic Subtropical Current afterward, and finally the North Equatorial current, which flows in a westerly direction towards the Caribbean Sea and the Gulf of Mexico. This turns around the North Atlantic Ocean gives rise to a movement known as the North Atlantic subtropical gyre. Additionally, other movements from other subregions are incorporated into and involved in this broad circulation. So, for instance, during the winter near the Iberian Peninsula, the atmospheric circulation close to the Iberian Peninsula diminishes and a poleward and along shelf flow develops entering the Gulf of Biscay, which is occasionally referred to as the Navidad current (Haynes and Barton, 1990). During the summer, winds blow along the African coast inducing the Canary Upwelling System and are southward along shore winds in the Iberian shelf inducing an upwelling regime in the Portugal and North Western Spanish coasts (Martínez et al., 2022).

Water circulation in the Bay of Biscay is well known and well reported in the literature (Friocourt et al., 2007; Charria et al., 2013; Solabarrieta et al., 2014; Basurko et al., 2022). The surface currents have a seasonal behavior strongly influenced by the wind (Solabarrieta et al., 2014). In winter, the current circulates eastward along the Spanish coast and northward along the French coast, while in summer, we find the counter current with an intensity three times lower (Charria et al., 2013), as shown in Fig. 1(b). All the water masses present in this region (and also along the Iberian west coast) come from the North Atlantic Ocean or from interactions between water masses from the North Atlantic Ocean and the Mediterranean Sea (Van Aken, 2001). The typical mean diameter of eddies in the Bay of Biscay is estimated at 45 km, and their occurrence shows seasonal variability, with a relatively large number of eddies in the first half of the year and relatively few eddies in the second half of the year. Friocourt et al. (2007) performed a Lagrangian numerical analysis to study the trajectories of the main water masses along the Bay of Biscay. Their study showed that the slope current system is responsible for an important part of the inflow and outflow of the Bay of Biscay.

The Mediterranean Sea is considered one of the main hotspots for plastics due to its closed nature (Tsiaras et al., 2021; Zambianchi et al., 2017). In addition to the influence of the Atlantic Ocean, the circulation within this sea has a very complex dynamic characterized by multiple gyres and eddies (Millot, 1999; Tsiaras et al., 2021). The influence of the North Atlantic currents and the bathymetry of the area also govern the circulation in this sea at different depth levels. Therefore, upwelling and downwelling processes also have a major effect on the surface circulation in the area (Peliz et al., 2007). In the southwest Mediterranean Basin, also known as the Alboran Sea, the dynamics are due to the mass intrusion across the Gibraltar Strait compensating for evaporation losses, but also to wind forcing. The surface circulation is mainly characterized by a frontal Atlantic jet water around two large-scale gyres, as shown in Fig. 1(c): the Western Alboran Gyre (WAG) and the Eastern Alboran Gyre (EAG). Abrupt changes in the WAG, including its collapse or eastward migration of the Atlantic jet, have been observed (Perkins et al., 1990; Flexas et al., 2006). In these situations, the Atlantic jet becomes a coastal jet that follows the African coast (Peliz et al., 2013). This mainly occurs during autumn and winter due to a dip in the inflow, giving rise to a seasonality in the surface circulation of the Alboran Sea (Vargas-Yáñez et al., 2002). This current is mainly formed by the Atlantic Waters in the surface and Levantine Intermediate Water in the subsurface (André et al., 2005). Based on several oceanographic campaigns, Alberola et al. (1995) described the seasonal variability mainly represented by a well-defined episode of narrowing, deepening, and offshore drift from late January to mid-March.

The hydrodynamic of the Gulf of Cadiz is complex, as described by Peliz et al. (2007) and Criado-Aldeanueva et al. (2009), since it is linked to that of the Mediterranean Sea. During the summer months, an anticyclonic pattern on the surface of the open sea favors the circulation towards the Strait of Gibraltar. For late autumn and early winter, the circulation shifts in a northwesterly direction, as shown in Fig. 1(c). Large-scale atmospheric models have concluded that wind influence is prevalent in the area. Particularly in winter, easterly winds (corresponding to a negative NAO value) cause local forcing (Criado-Aldeanueva et al., 2009).

Regarding the Canary Islands, the oceanic dynamics in this region are characterized by subtropical gyres. Vélez-Belchí et al. (2017) demonstrated that there is an intense seasonal cycle in the south of these islands. Their results showed that there is a significant difference in transport between spring and fall. For the surface waters and the North Atlantic Central waters, there is a change in intensity and a slight variation in the location of the main water mass transport.

3. Numerical methods

3.1. Lagrangian model

The MOHID-Lagrangian model (Sobrinho et al., 2023) was used for the computational simulations. It has been widely used to describe the behavior of marine debris at sea, as well as other floating objects. Developed within the MOHID modeling system (Campuzano et al., 2016), this tool is a complete, high-resolution Lagrangian tracking model that can function as a library for the MOHID Water modeling system or as a stand-alone program.

A previous study developed by Cloux et al. (2022) tested the reliability of the model by comparing simulation data with beach monitoring data from Ria de Arousa (Galicia, NW Spain). The model was used to track the transport of marine debris over time in the Rias, and estimate its accumulation along the Galician coast. Despite the increasing availability of in situ monitoring data, this information hardly explains the trajectory and origin of marine litter but simply indicates the areas where it is found at a given time and where it may accumulate (the fate). Currently, the only way to estimate the transport, accumulation, and/or dispersion of marine litter is through modeling tools, i.e., through mathematical equations that parameterize the behavior of particles in the sea. The model describing the kinematic motion of the particles can include, besides currents, other effects such as wind, waves, and diffusion. Then, from a Lagrangian point of view, the particles position is given by,

$$\frac{dr_i}{dt} = v_i(r_i(t), t) + R\sqrt{\frac{2K_h}{\Delta t}} \tag{1}$$

where v_i represents the particle's velocity interpolated from the flow field at the particle position r_i and time instant t. The last term is a random component that must be added to the particle motion to consider higher resolution turbulent effects that are not represented in the resolution at which the simulation is performed (Lebreton et al., 2012; de Pablo et al., 2022). R is a random number from a continuous uniform distribution with zero mean and standard deviation of 1. The parameter $K_h = 1\ \mathrm{m^2 \cdot s^{-1}}$ is the turbulent horizontal diffusion coefficient. The velocity of the particle v_i can be expressed as the sum of several contributions concerning different effects, since the size, density, and buoyancy of the body being simulated can vary, which influences the type of phenomena that affect its movement. For example, if we simulate a particle with buoyancy, the body fraction above the surface will be affected by the wind. In the particular case of the study presented here, we are considering purely surface Lagrangian particles to simulate the motion of plastic debris on the surface; therefore, we have only used the hydrodynamical contribution, and extra forcing on potentially emerged parts of the debris is neglected.

Plastic debris may reach land and beach on the near-shore. To this end, for the study area the model includes a land interaction mask (LIM) which is obtained from the grid considered by the model. Therefore, it respects the size of the original grid. This mask can differentiate between four values, which are in the range of −1 to 2, and their value categorizes the type of terrain considered in each cell. Non-missing value[1] cells are considered water (w_c), missing value cells are considered land (l_c), cells adjacent to missing cells above a set threshold height are considered beach cells (b_c), and cells below that threshold are considered seabed cells (d_c). Cell values are categorized as it is shown in Fig. 3(a). The threshold is set by the user in the simulation settings, which is particularly useful depending on the terrain and the retention capacity of the area. In our study, we must select a threshold value that is representative across the entire global domain. Considering the bathymetric profile of the western European coast and the average tidal coefficients, we have established a threshold value of −3.5 meters.

Beaching occurs when a particle arrives to beach cells $LIM = 1$, as shown in Fig. 3(b). Then, the particle may (i) stop (its current speed is reduced to zero) if a randomly generated number (between 0 and 1) is less than the beaching probability r_w or (ii) continue to move into the beach with a velocity reduction factor,

$$f_v(LI) = b_w(LI) \cdot r_w \tag{2}$$

with b_w a beach quadratic weight in the range [0,1] that weights how deep a particle is in a beach cell,

$$b_w(LI) = 1 - \left(\frac{LI - b_{min}}{b_{max} - b_{min}}\right)^2 \tag{3}$$

$b_{min} = (w_c + b_c)/2 < LI(t) < b_{max} = (b_c + l_c)/2 \quad (0.5 < LI(t) < 1.5)$. The Land-Interaction state $LI(t)$ of each beached particle is linearly interpolated between b_{min} and b_{max} depending on the particle position within the beach cell. The procedure is repeated for each iteration step until the particle hits land, where it definitely stops. The particle may return to water cells during the time it spent traveling through a beach cell.

This way, it is possible to set a threshold depth value above which the particle may become stranded, as well as a probability for particle beaching. With these parameters, different accumulation scenarios can be modeled. Cloux et al. (2022) observed that in much of the cases the influence of the beaching factor for the Lagrangian transport is negligible while in other cases, the real exposure to the beach may not be well described in the simulation. Beaches may have a complicated orography (stones, algae, etc) that can influence the retention of floating particles, and these may not be well reproduced in the simulated coastline. However, Cloux et al. (2022) could not establish a linear relationship between the beaching factors that fit well with all kind of beaches. Future versions of MOHID-Lagrangian model will include more complex formulations to reproduce the washing-off by tides and waves.

For this study, two 7-year simulations were performed between January 2015 and December 2021 to obtain high statistical significance. Simulations were performed with a spatial resolution of 9 km to align with the original grid size and a temporal resolution of 4 h, but model outputs are averaged to 1 day. This time resolution was used to avoid tidal coupling and keep the simulation computationally reasonable. The first obtained results do not consider any beaching factor, so it only includes fluid particles that move through the study domain but are not trapped on the coast. In the second simulation, a $r_w = 50\%$ beaching coefficient has been introduced to study the impact of this factor on dispersion. This is an arbitrary choice to avoid considering retention that is either too high or too low. The influence of rivers and on-land sources has been studied. Each type is described in detail in the following subsection. For this purpose, we used a grid covering the marine demarcations of the North Atlantic Ocean (with a resolution of 0.5°). As we are not only interested in the dispersion of plastics in the Atlantic, but also in specific areas, we also used a higher resolution grid of the Bay of Biscay, the Alboran Sea and the Mediterranean Sea (each with a resolution of 0.25°).The concentrations obtained are described in terms of the number of particles per unit area. Concentration values estimated for the entire period in each cell have been normalized with respect to the total number of particles emitted during the 7-year simulation N_{tot}. Thus, the relative accumulation (RA_c) inside the grid cell c has been calculated as follows,

$$\%RA_c = 100\frac{\sum_t N_c(t)}{N_{tot}} \tag{4}$$

3.2. Input data

The MOHID-Lagrangian model has been forced with hydrodynamic Eulerian fields. Hydrodynamic data is obtained from the Operational

[1] Missing value cells refer to mesh points outside the calculation domain.

Mercator global ocean analysis and forecasting server (Copernicus, n.d). This operational model provides 3D mean daily files of temperature, salinity, currents, and sea level, among others, with a spatial resolution of 0.083° for mixed layer depth and top-down ice parameters over the global ocean. It also includes hourly mean surface fields for sea level height, temperature, and currents. The 50 vertical levels range from 0 to 5500 m, but only the surface level is used in this study. Rivers outflows are taken into account in the operational model by Mercator. Additionally, this product provides a unique dataset for surface currents, which includes wave and tidal drift, known as SMOC (Surface Merged Ocean Current). SMOC calculates the total surface current by combining contributions from the general oceanic circulation, tides, and waves. The Stokes current resulting from wave motion alone can account for up to half of the surface drift when strong wind and waves are present. SMOC data are computed daily, using one day of hindcast for the previous day, and five days of forecast ahead from the date of production. It's crucial to note that while the SMOC product, which integrates surface wind, has been utilized to estimate currents, the Lagrangian model itself does not incorporate wind fields to estimate trajectories, since we assume that debris particles are fully submerged in the water. Only the first 24 h of forecast are used for daily simulations.

3.3. Emission sources

Despite the fact that in recent years efforts have been made to standardize monitoring methodologies or to relate the emission rates and destinations of plastic debris in the ocean (van Duinen et al., 2022), currently it is still impossible to obtain complete information, continuously in space and time, on the points and rates of emission of terrestrial trash that ends up in the sea. Therefore, in marine litter modeling work it is necessary to make assumptions to define emission concentrations (number of particles emitted per unit of time) and consider the results in relative terms. It is commonly believed that most plastic waste comes from land-based sources, especially from densely populated inland areas, although some studies suggest that marine sources also contribute significantly. However, there is a significant discrepancy between the estimated amount of land-generated plastic waste entering coastal waters (Cozar et al., 2014; Van Sebille et al., 2015) and the estimated total amount of plastic actually observed at sea (Jambeck et al., 2015). This indicates that our understanding of the movements, routes, and fate of plastics is still incomplete. When and how these emissions are released is still a puzzle for the scientific community. All of this makes the determination of emissions a challenging process, and therefore the results must be carefully considered.

In the MOHID-Lagrangian model, emissions are characterized by location, release time, and emission rate. Usually, the release time of the emission coincides with the initial instant of the simulation, and the rate allows us to control how the particles are emitted. In this study, both a continuous emission rate and a time-varying emission rate are considered. Three regional emission sources have been considered in this study as shown in Fig. 2(b); Cantabrian sea (R1), Gulf of Cádiz (R2), and Canary islands (R3). Besides, two kinds of particle sources were considered; (1) river discharges, which are reported to be the main route for waste to enter the oceans from land sources (González-Fernández et al., 2021); and (2) on-land emissions, which regards areas with a higher probability of acting as sources of marine litter such as population centers, ports, bathing areas, and solid urban waste dumps.

For the river emissions, 27 rivers along the Atlantic Iberian Peninsula coastline have been considered. Given the impossibility of determining the exact quantity of plastic released and the timing of these emissions, it can only be assumed that the emissions will correlate with the river's flow; thus, higher flow rates would likely result in greater contributions to marine debris. They are distributed among 6 River Basin Districts (RBD) that flow into the Atlantic Ocean: Eastern Cantabrian, Western Cantabrian, Galicia-Costa, Miño-Sil, Guadiana, and Guadalquivir. The emission rates assigned to these sources follow the flow values obtained from historical gauging records of the monitoring networks (https://sig.mapama.gob.es/redes-seguimiento/). Variable rate emissions correspond to recorded river discharge flow. Daily flow data were used in the model. Due to the unavailability of data at this frequency for some rivers, the mean flow for the month was used as the daily flow. In cases where no data were available for the corresponding month, the monthly mean flow of the time series was used.

A total of 2.7 million particles ($N_{tot} = 2.7{\cdot}10^6$) were emitted from rivers along the 7-years simulation period. The emission points were chosen based on the locations of the mouths of each river, Fig. 2(a). According to Lebreton et al. (2017), hydrological information should be complemented by other effects affecting the entry of plastics into the ocean, such as management and plastic waste or population density around the river basin, as well as anthropogenic structures that act as transport barriers. For this reason, river flow values are also weighted in agreement to González-Fernández et al. (2021) (see Appendix A for details). In this work, the authors made different visual records of floating macroplastics in 42 European rivers between June 2016 and

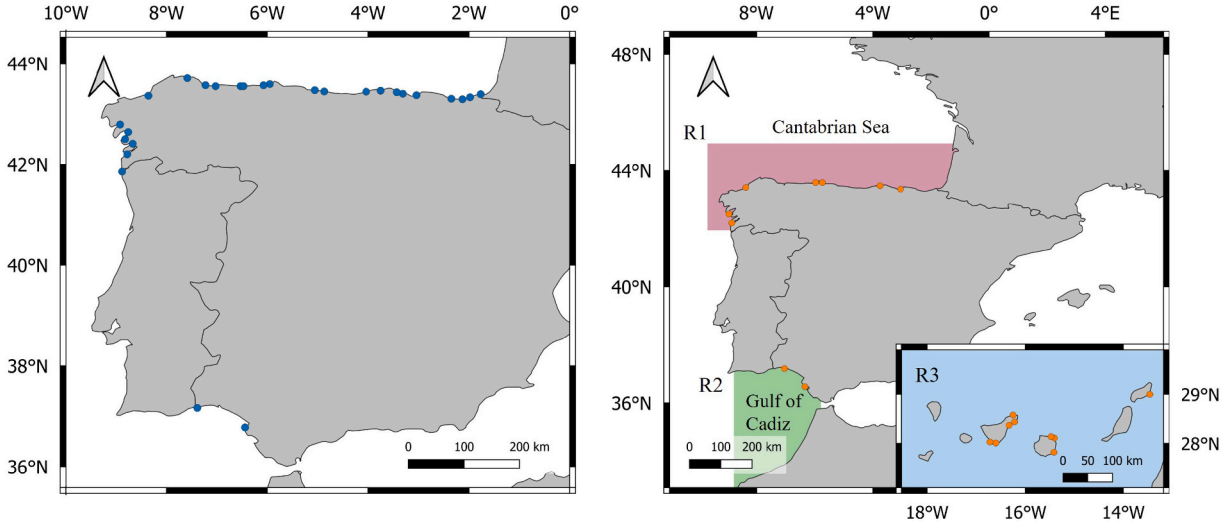

Fig. 2. Western Atlantic Spanish emission sources considered in this study: (left) 27 mouth rivers (blue dots), and (right) 18 on-land points (yellow dots). The three source regions considered in the study are shown in the right panel: R1, Cantabrian Sea region (red shadow), R2, Gulf of Cadiz region (green shadow) and R3, Canary Islands region (blue shadow). (For interpretation of the references to colour in this figure legend, the reader is referred to the web version of this article.)

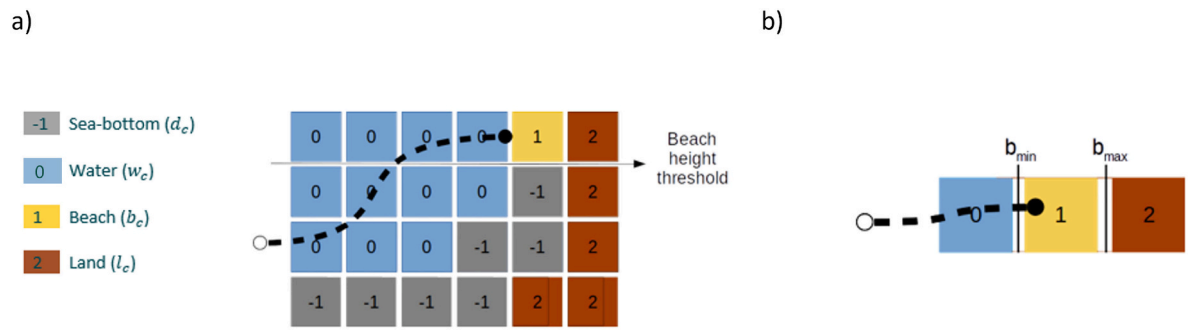

Fig. 3. Beaching process implemented in MOHID-Lagrangian model. a) Assignment of the Land-Mask Interface values (LIM). b) Beaching scenario where a particle moves from water to beach. (For interpretation of the references to colour in this figure legend, the reader is referred to the web version of this article.)

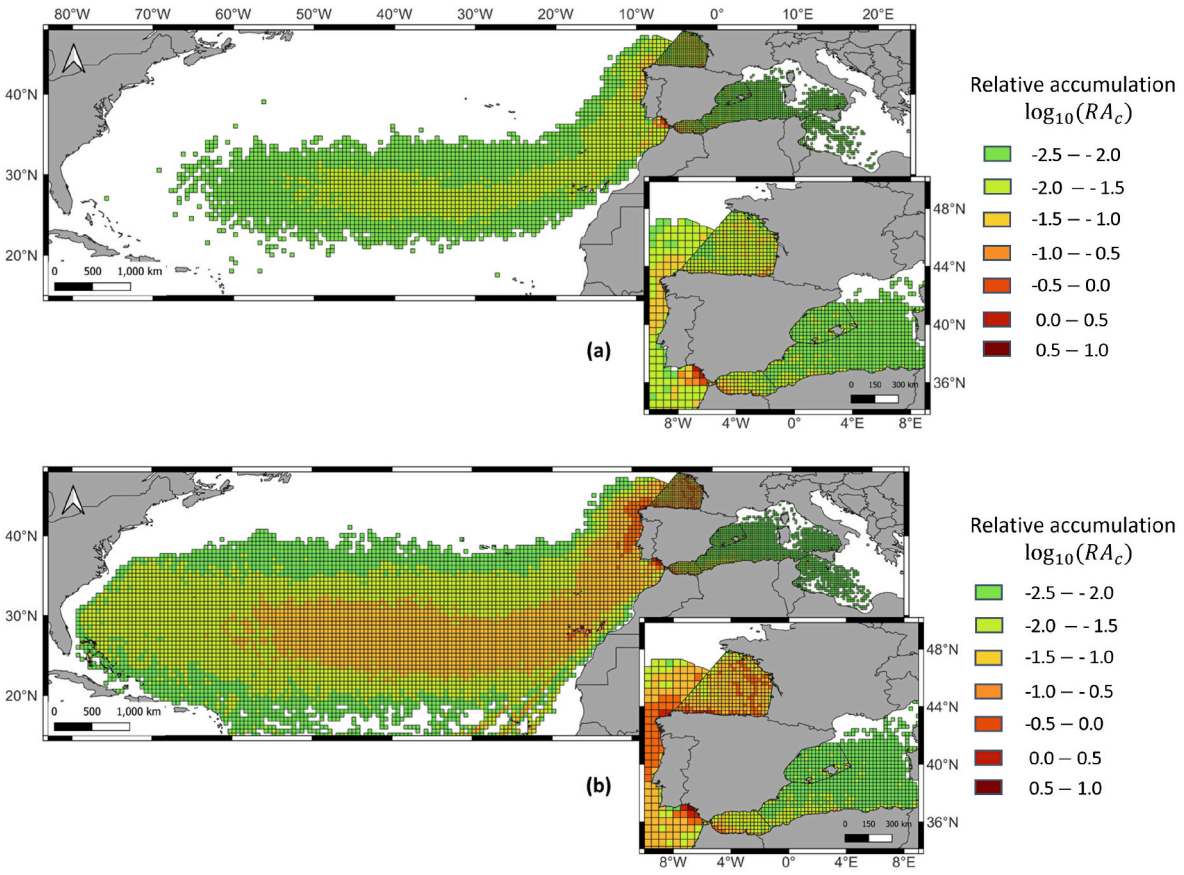

Fig. 4. Global relative accumulation in the North Atlantic Ocean for rivers (a) and land (b) emissions. The ratio of the number of particles that crossed each cell during the whole simulation period to the total number of particles released is represented by the logarithmic colour bar in percentage form. (For interpretation of the references to colour in this figure legend, the reader is referred to the web version of this article.)

September 2017. Thus, the authors created a regression model with these results and the characteristics of the basin (size, number of inhabitants and estimation of waste escaping from the collection system in that basin) to estimate the relative contribution of each river on the European coast to floating marine litter.

Regarding on-land emissions (harbors, beaches, urban solid waste landfills, and other potential points), the Pressures and Impacts Analysis of the Marine Strategy was used (MAPAMA (Ministerio de Agricultura y Pesca and Públicas), 2012a,b). In this work, a mapping and assessment of the accumulation of pressures that can cause the entry of garbage into the sea from land was carried out for regions R1 to R3. In this analysis, scores from 1 to 10 (higher score as the number of pressures and/or their magnitude increased) were assigned to each 10 km coastal cell. To select the emission points, the areas with the greatest accumulation of pressures were searched (those with cells whose scores were among the three highest in the district) and a unique emission point representative of each of those was determined, resulting in 18 emission points (see Fig. 2 (b)). It should be noted that, within the area covered by these cells with higher pressure, the exact location of the emission point is not relevant to the scale at which the simulations are being carried out in this work (demarcation scale, with a resolution of 8 km). Regarding the emission rates (see Appendix A for details), these were weighted and normalized based on the score assigned (MAPAMA (Ministerio de Agricultura y Pesca and Públicas), 2012a,b), and 2.5 million particles ($N_{tot} = 2.5{\cdot}10^6$) were emitted along the 7-years simulation period.

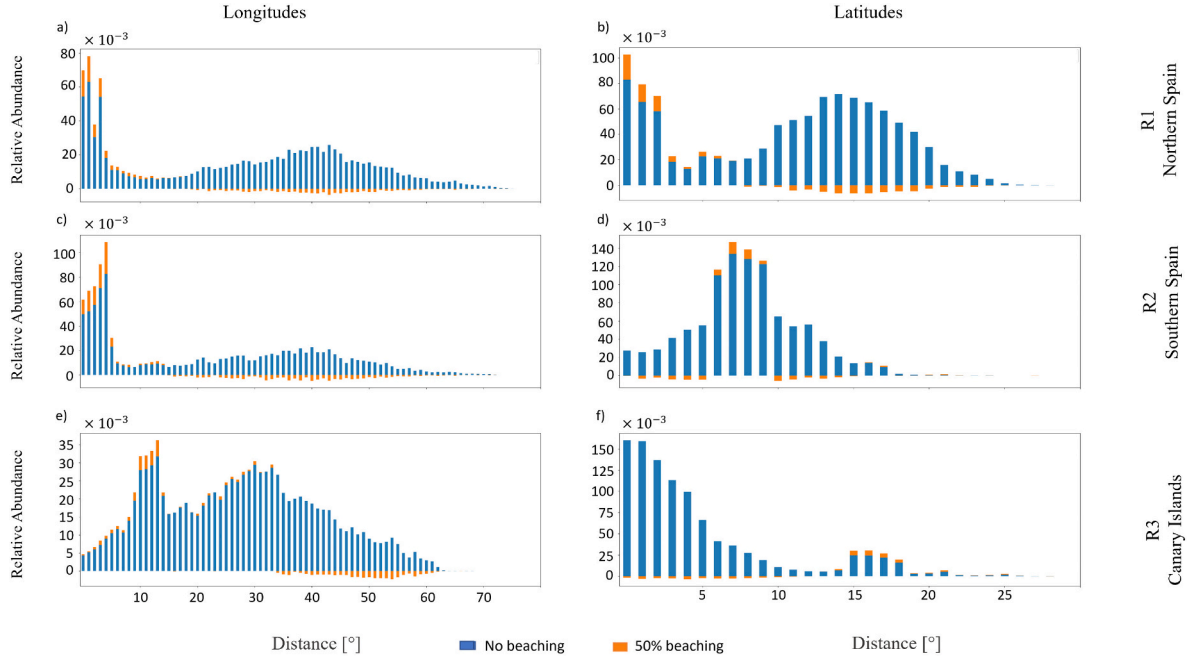

Fig. 5. Longitude (left column) and latitude (right column) dispersion for rivers and on-land emissions grouped by regions: (a,b) Northern Spain, Cantabrian sea (R1); (c,d) southern Spain, Gulf of Cádiz (R2); and (e,f) Canary Islands (R3). Blue and orange bars correspond to results without and with beaching (50 %), respectively. Note that the y-axis limits may differ in some graphs. (For interpretation of the references to colour in this figure legend, the reader is referred to the web version of this article.)

4. Results

4.1. Concentrations

The relative concentrations of macroplastics in the North Atlantic Ocean over a 7-year period for rivers and on-land sources are shown in Fig. 4. Beaching processes are not included in this analysis. Particle concentrations in each cell are shown as a percentage of the maximum accumulation value obtained for each type of source (RA), Eq. (4). Values below 0.1% have been omitted in this representation. Accumulation results were categorized using a logarithmic scale, $log_{10}(RA_c)$.

Plastic emissions from Spanish coasts reach the north Atlantic waters although the concentration values for the plumes observed in Fig. 4 are quite small if compared to the values registered near the coast. Concentrations values due to on-land emissions (Fig. 4b) in some location in the open sea are larger than those due to river emissions (Fig. 4a). River emissions occur mainly during autumn and winter seasons, coinciding with the largest precipitation values and outflows, thus driving the waste farther from the coast than on-land emissions, increasing the probability to be transported by currents. On-land plumes are wider than rivers ones probably due to their constant emission.

In the north of Spain, accumulations in the Bay of Biscay become more notable, with larger concentrations appearing parallel to the French coast (Declerck et al., 2019). The highest accumulation records appear on the Spanish side, although significant values were observed also in French waters. The semi-enclosed nature of this region favors particle retention (Basurko et al., 2022). The northwestern part of the Peninsula also shows high concentration values near the coastline due not only to the presence of local rivers but also to the westerly winds and the Iberian Poleward Current. Despite having fewer emission points, the Cantabrian coast registers higher values than in the previous case for the entire coastline. This is also observed on the Galician coast (NW of the Iberian Peninsula). For river emissions, the highest concentration is recorded in the south of the peninsula, in the Gulf of Cadiz. This result is consistent with the large contribution of the Guadiana and Guadalquivir rivers, the largest rivers considered in this study, according to González-Fernández et al. (2021). Note that the accumulation zones are also displaced towards the Alboran Sea. In this area, the highest values are assigned to the northern coast of Morocco, which is coherent with the circulation in this area. The presence of eddies and their weakening and collapse favor the accumulation of particles in the Mediterranean coast of Morocco. The Canary Islands are apparently not significantly affected by pollution produced by peninsular rivers. These results suggest that pollution governed by rivers flows may be widespread, but it is more significant at the local scale. New accumulation areas also appear around the Canary Islands as some emission sources were located in this archipelago. This, again, indicates that the observed plastic contamination remains mainly local near the coastline.

4.2. Dispersion

To study the dispersion of particles in latitude and longitude, both rivers and on-land emissions are grouped into three regional areas as shown in Fig. 2(b): R1, covering the north coast of the peninsula, R2, covering the Gulf of Cadiz, and R3, covering the Canary Islands. The dispersion of particles related to the emitter location is determined for each individual source. The position of the particles emitted from point sources at their final state after 7 years of simulation was recorded. The dispersion is then obtained as the difference between the final and initial position. Fig. 5 shows the obtained results for longitudes (left column) and latitudes (right column) for the three considered regions. The results are presented as a normalized histogram to show the distribution of particles dispersion. The blue bars correspond to the results without a beaching coefficient, i.e., particles that flow without being retained on the shore, and the orange bars show the differences by assuming 50 % beaching. At longitudes and latitudes where the accumulation increases, the difference is represented by an orange bar added above the blue one, while for cases where the concentration decreases, the bar is added below the blue one.

R1 considers all sources located in the north of the Iberian Peninsula. The highest concentration of Lagrangian particles is found at short distances, both in latitude and longitude (below 10° on longitude and 5° on

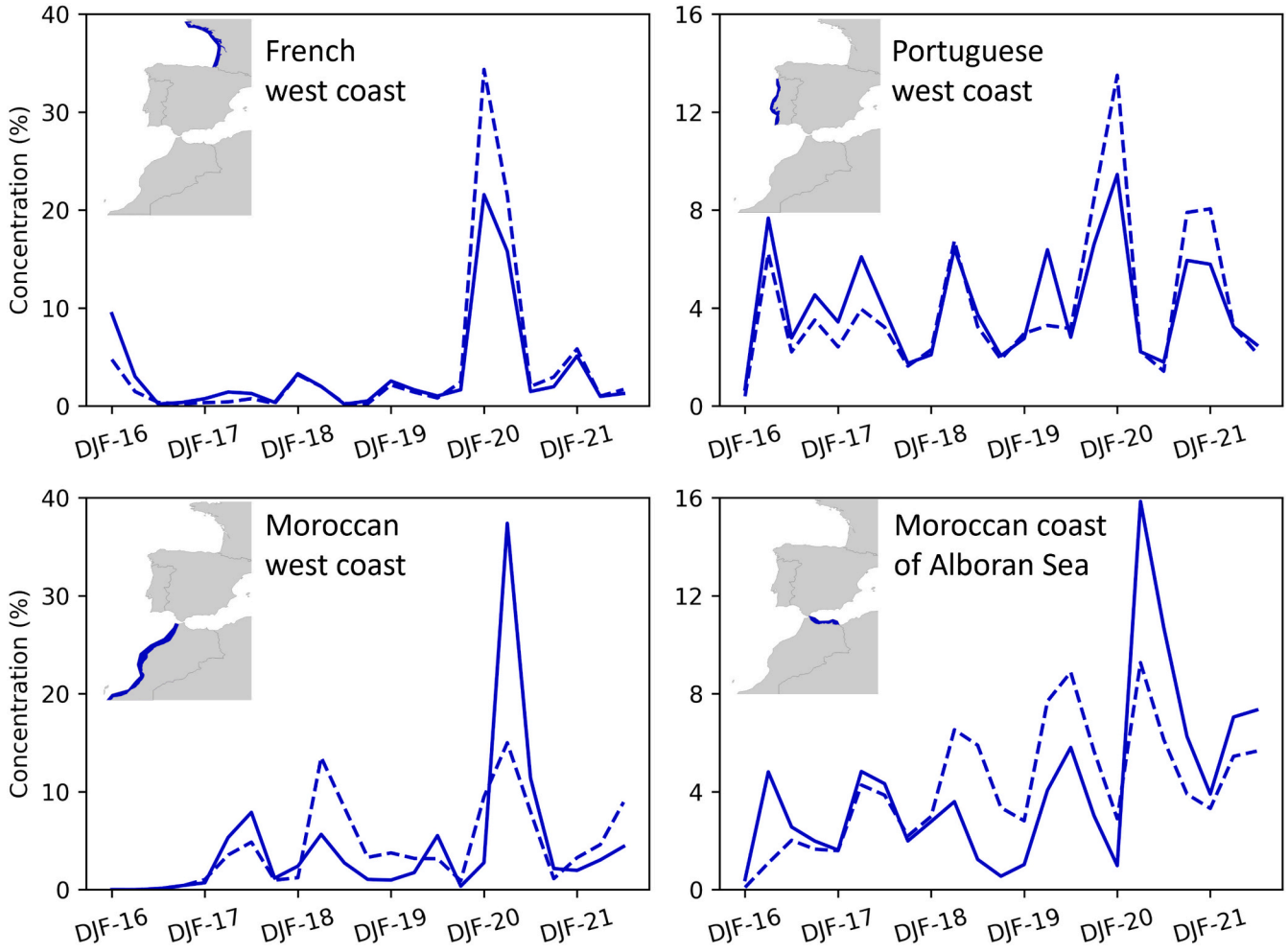

Fig. 6. Time series of plastic concentrations reaching the coasts of France, Portugal, western and Alboran coasts of Morocco. Solid and dashed lines correspond to contributions from rivers and on-land emission Spanish sites, respectively. The ratio of the number of particles from all the rivers and on-land locations along the Atlantic Spanish coast that reached the surrounding coasts over the entire simulation period to the total number of particles that reached those coasts is shown as concentration percentages. Only x-ticks for the winter seasons are shown. Note that the y-axis limits may differ in some graphs.

latitude). With major distribution values seen within the first five degrees of both longitude and latitude, particles tend to accumulate close to the emission locations. This effect is enhanced considering the beaching effect. There is also noticeable distribution at medium distances, but it is reduced when beaching is considered. As described above, the dynamics of the Bay of Biscay differ between winter and summer seasons. The semi-enclosed nature of the region favors the retention of particles (Basurko et al., 2022). For the particles emitted close to the corner of the bay, a greater distribution of particles is observed in the near longitudes and latitudes than in the case of sources located further west. Emissions closer to the Atlantic Ocean experience greater dispersion towards middle distances in the warm seasons. This is due to the westward flow during this time of the year, and this seasonal effect is confirmed in the next section of this study.

For the Gulf of Cadiz (R2), the nearest longitudes, below 5°, had the maximum particle concentration. Latitudinally, the medium distances show a large concentration of particles, particularly in the 5 − 10 degree range from the emission points, whereas the near and far distances are less significant. This behavior is reinforced by the beaching process. The semi-enclosed nature of the Gulf of Cadiz results in the retention of particles in the region, which is consistent with the circulation patterns in the area. Regardless of the time of the year, the circulation flows around the coast, towards the south (Moroccan coast) in winter and towards the north (Spanish coast) in summer.

Regarding the Canary Islands (R3), a larger dispersion is observed at mid and far longitudes, while the opposite is observed in terms of latitude dispersion, as the region is under the influence of the Canary Current (dominant north-south direction). Not seeing concentrations at the local scale is to be expected, as this archipelago experiences strong oceanic dynamics that influence dispersion at the scale we are considering. This dynamic is responsible for the transportation of water masses from the west of the peninsula to tropical and subtropical longitudes, and towards the east coast of the Americas. So there is more dispersion in terms of longitudes (around 25–40°). On the other hand, a large latitudinal dispersion will not occur, since the maximum dispersion is around 3°.

4.3. Seasonality and transboundary pollution

To analyse the transboundary contribution of plastics from the Spanish coast, time series of relative contributions (%RA), with groupings of seasonal (quarterly) results over a seven-year simulation period, were analyzed, in a region of the French coast, the Portuguese mainland coast, the Moroccan west coast and the Moroccan coast located in the Alboran Sea (Fig. 6).

Concentration densities were calculated considering a 50 % probability of beaching. Considering simulations without stranding probability does not significantly change the percentage contributions of each

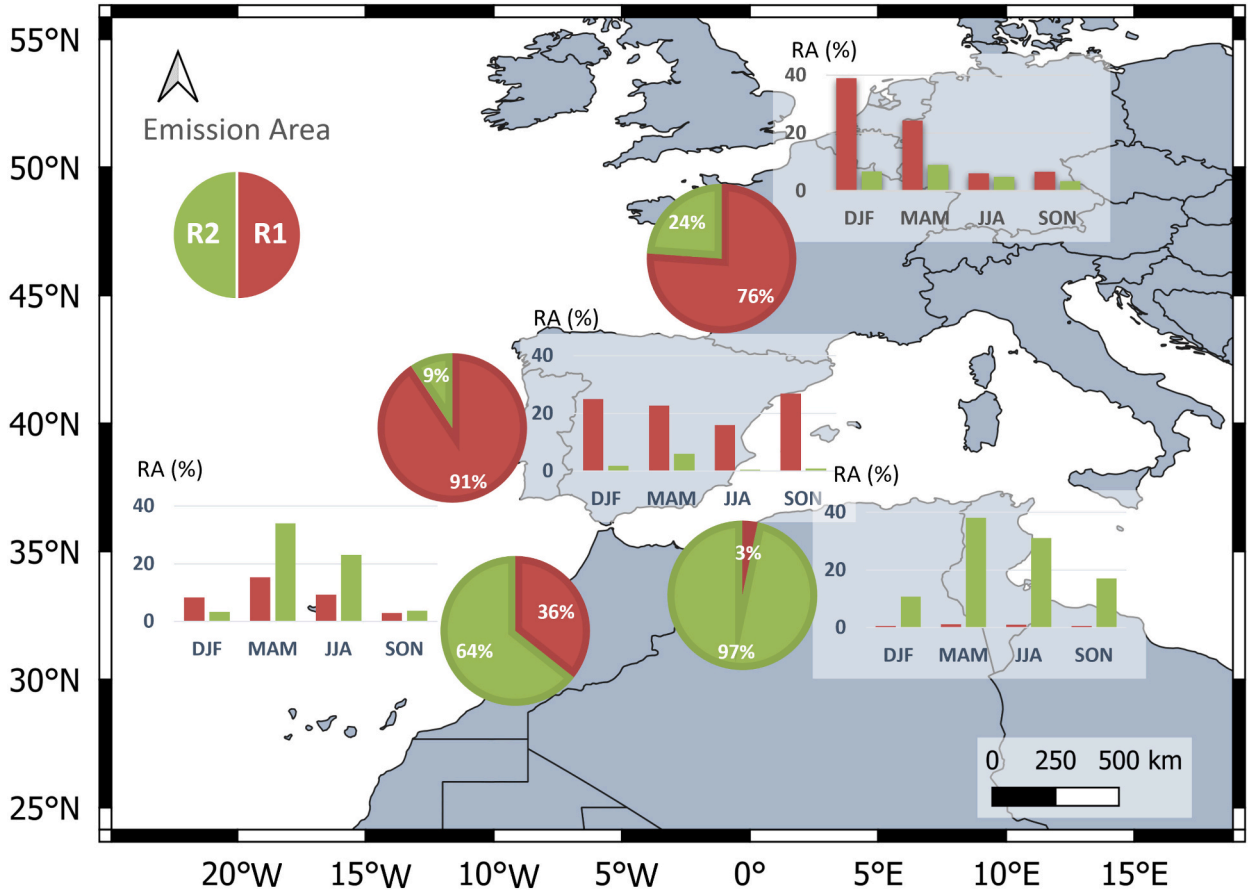

Fig. 7. Spanish contribution of plastic pollution to the neighboring countries shown as pie charts and the seasonal evolution of the most significant sources in bar charts. Concentration percentages are shown as the ratio of the number of particles that reached the neighboring coasts from the north of Spain (R1) and the Gulf of Cadiz (R2) during the whole simulation period to the total number of particles reaching those coasts. R1 and R2 sources are shown in red and green colors, respectively. The contributions of R3 are negligible. (For interpretation of the references to colour in this figure legend, the reader is referred to the web version of this article.)

region. The largest concentrations on the French coast are observed during the winter months (December, January and February), coinciding with river flooding periods. With a consistent delay that corresponds to the time it takes for particles to travel there, this phenomenon is also seen in the Portuguese region. The coasts of Morocco and Alboran also experience this growth during the cold seasons. However, the periodicity is more pronounced on the Moroccan coast of the Alboran Sea. This phenomenon may be closely linked to the combined dynamics of the influx of water masses from the Atlantic along with the WAG and EAG. It should be highlighted that Spain experienced heavy precipitation episodes at the end of 2019 and the beginning of 2020, which boosted the contribution of fresh water from rivers to the transport of plastics on the surface dragging marine litter from rivers and on-land sources. The contribution of the Guadalquivir River is especially significant as shown by the largest peak on both Morocco coasts.

The relative transboundary contribution of the Spanish on-land and river emissions for the entire simulation period (pie charts) and seasonally grouped (bar charts), is shown in Fig. 7. In terms of the number of particles reaching each coast, the contribution of particles from R1 (northern region) on the French coast is 1.3 times that of the Portuguese coast, while the contribution of particles from the R2 region (Gulf of Cadiz) is 4 times higher. This demonstrates that the east Bay of Biscay is a dead-end for plastics (Basurko et al., 2022), contrary to the Portuguese coast which is "periodically washed" by the westerly winds and the rivers outflows. As a result, resident times are influenced by the wind and surface current speeds, as high speeds would significantly shorten the residence times of plastics. Therefore, it would be reasonable to anticipate low/high concentrations of litter in areas with high/low dynamics, respectively. Finally, the contributions of R1 and R2 regions on both sides of the Morocco coast behave as expected from previous results shown above; R1 contributes much less to the Alboran sea as most of the macroplastics are carried out by the North Atlantic current and then by the Canary Current until they meet the Equatorial Current, where the dominant direction is westwards. Note that R3 region (Canary islands) contribution is negligible for all the countries, except for the western coast of Morocco (1 %, not shown in the graph), due to its proximity to the Canary Islands. Observe that, contrary to what might be anticipated given its remoteness, the Gulf of Cadiz contribution is substantially higher for the French coasts than for the Portuguese.

Considering the seasonal behavior, note that most of plastics reaching the western coast of France occur during winter (December, January, and February) and spring (March, April, and May) due to a predominant anticyclonic current flowing from west to east and northward along the marine shelf off the coast of France (Declerck et al., 2019; Basurko et al., 2022). However, in summer (June, July, and August), the transport of particles from R1 to the French coast diminishes as the opposite current motion (cyclonic) appears three times less intense. An increase of particles from R2 was observed during the spring on the Portuguese coast as a consequence of the decrease in the intensity of westerly winds and a decrease in the flow of the Atlantic jet. On the other hand, R1 and R2 particles reaching the western and north coasts of Morocco increase during the spring and summer months, coinciding with the motion of surface currents in an easterly direction towards the Strait of Gibraltar. The increased inflow of water through

the strait reinforces the Western Alboran Gyre (WAG) and thus the particle beaching. For late autumn and early winter, a sharp decrease is observed due to the weakness of the Atlantic current entering this area.

5. Conclusions

The dispersion and accumulation of plastics in the open seas is a global problem that needs to be urgently addressed. In this work, a Lagrangian statistical study is presented to estimate the potential accumulation areas of floating plastics in the North Atlantic Ocean. For this purpose, the Lagrangian tool MOHID-Lagrangian has been used, considering two-type emission sources, rivers and on-land, and three regions of emissions (north of Spain, Gulf of Cadiz and Canary islands) in the Spanish coasts. For each source separately, a 7-years simulation has been run. Neutrally buoyant litter was supposed to behave as Lagrangian tracers that are transported only by surface currents.

According to our findings, continuous emissions of plastic on land tend to remain closer to shore and in higher concentrations compared to intermittent emissions from rivers, which are flow-dependent. Concentrations of land-based plastic in the North Atlantic Ocean are higher than those of plastics emitted from rivers. Plastic emissions from the Spanish coasts reach the waters of the North Atlantic, although the concentrations of these plumes are relatively small compared to the values recorded near the coast. Emissions from rivers occur mainly during the autumn and winter seasons, coinciding with the highest precipitation and flow values (as shown in Fig. 6), increasing the probability of being transported by currents. Land-based plumes are wider than river-based plumes, probably due to their constant emission.

Particularly, and regardless of whether we consider time-dependent (rivers) or continuous (on-land) emissions, accumulations in the Bay of Biscay are more pronounced. On the Spanish coastal side, the highest accumulations have been reported, although notable amounts are also found in French waters. The semi-enclosed geography of the region encourages particles to be trapped, and westerly winds and the northward current along the Iberian Peninsula also have an influence. For river emissions, the highest concentration is recorded in the south of the peninsula, in the Gulf of Cadiz, in line with the large contribution of the Guadiana and Guadalquivir rivers. The accumulation areas also move towards the Alboran Sea, where the highest values are found on the north coast of Morocco, according to the circulation in this area. The presence of eddies and their weakening and collapse favor the accumulation of particles on the Mediterranean coast of Morocco. The pollution from peninsular rivers does not appear to have a significant impact on the Canary Islands. These findings indicate that although pollution caused by river flows from the peninsula is widespread, it has a more significant impact at the local level. When analyzing land-based sources, it has been found that there are new accumulation areas around the Canary Islands, as some emissions sources are located within the archipelago. This suggests that the plastic pollution that has been observed is primarily concentrated near the coastline.

Relative accumulation maps provide a good initial approximation, but they do not provide detailed information on the dispersion of Lagrangian particles in the open ocean. To better understand particle dispersion, the final positions of particles have been used to calculate relative dispersion in both latitude and longitude for rivers and on-land sources. An arbitrary beaching factor (50%) was considered to take into account the possible influence of retention on the dispersion of particles. As a function of the emission source, for the northern peninsula, particles tend to remain in the neighborhood locations, with major distribution values found within the first five degrees of both longitude and latitude. This effect is enhanced when beaching is considered. Particles emitted from the Gulf of Cadiz do not disperse in longitude (below 10°) due to the dynamics of the region, but they are significantly dispersed in mid-latitudes (between 5 and 10°). Once again, the consideration of the beaching factor reinforces this behavior. Finally, for emissions from the Canary Islands (R3), the dispersion of particles follows the circulation in the region. The Lagrangian particles simulated in this zone are transported to a greater extent towards tropical and subtropical latitudes (causing a lesser dispersion in latitudes, mostly below 5°) and the east coast of America (above 10° and up to 50° at longitude), following the Canary Current and the north equatorial current.

Particles that arrived in France, Portugal, and Morocco predominantly originate from the Cantabrian coast and the Gulf of Cadiz, highlighting the transnational nature of the issue. The relative concentration of litter coming from the Gulf of Cadiz is higher on the French coast than in Portugal. This is due to the morphodynamic conditions of the Bay of Biscay and to the fact that the Portuguese coast is periodically washed by the northwest winds and rivers outflow. On-land emissions from the Canary Islands only contribute to 1 % of the concentration measured in the western coast of Morocco despite its proximity. Finally, we observed that a high seasonal variability dominates the Lagrangian dynamics and plastics tend to arrive to other countries mainly during winter season due to the meteo-oceanographic conditions.

As future work, other factors that can impact particles transport, such as windage, Stokes drift, and bio- fouling, among others, must be taken into account. These studies are of great interest because degradation processes may modify substantially the shape of the plastic debris affecting their trajectory. A valuable direction for further research would be to conduct a study examining the age of the particles, specifically to investigate the relationship between accumulations near the ground and the particles released either at the beginning or the end of the simulation. A 3D study is also crucial, as it has been observed that plastics move vertically and may experience settling and refloating phenomena. Besides, to account for local currents that may change the final beaching of plastics, higher resolution atmospheric and hydrodynamic models should be used to focus on coastal accumulations, and emission rates should be better characterized because they have a significant impact on the outcomes.

CRediT authorship contribution statement

Sara Cloux: Writing – review & editing, Writing – original draft, Software, Resources, Formal analysis. **Patricia Pérez:** Writing – review & editing, Resources. **Hilda de Pablo:** Writing – review & editing, Supervision, Project administration, Methodology, Funding acquisition. **Vicente Pérez-Muñuzuri:** Writing – review & editing, Supervision, Project administration, Funding acquisition, Conceptualization.

Declaration of competing interest

The authors declare that they have no known competing financial interests or personal relationships that could have appeared to influence the work reported in this paper.

Acknowledgements

We gratefully acknowledge financial support by CleanAtlantic and FreeLitterAT Interreg Atlantic Projects (EAPA 46/2016 and EAPA-0009/2022) and Xunta de Galicia under Research Grant No. 2021-PG036-1. P. Pérez was funded by the 6-ESMARES2-C8 project, which is supported by the Spanish Ministry for the Ecological Transition and Demographic Challenge. Financial support by the Galicia Marine Science programme included in the Recovery, Transformation and Resilience Plan (PRTR-C17·I1) is also acknowledged.

Appendix A. Emission rates

The number of plastic debris emitted by rivers is calculated as a function of the rivers outflows. To that end, for each river we obtain from González-Fernández et al. (2021) a factor f related to the number of plastic items emitted per year. A weighting factor for each river j is calculated as,

$$w_j = \frac{f_j}{min_j\left(f_j\right)} \tag{A.1}$$

and the number of released particles per month and river is obtained as,

$$N_j^t = N_{tot}\frac{w_j Q_j^t}{\sum_j\left(w_j\sum_{t=1}^{M} Q_j^t\right)} \tag{A.2}$$

with M the total number of emission time steps considered, and Q_j^t the monthly mean flow.

As an example, Tables A.1 and A.2 show the weighting factors, monthly mean flows and number of particles released per month for three Spanish rivers during one year. For simplicity we assume for this example that $N_{tot} = 100000$.

Table A.3 shows the monthly emitted particles from land sites. Weighting factors were obtained from MAPAMA (Ministerio de Agricultura y Pesca and Públicas) (2012a,b). As for the rivers case, we assume a total of 100,000 particles emitted along the year, equally distributed by month, and weighted by a factor ranging from 1 to 6. Land particle emission is maintained constant along the simulation. Thus, the fifth column in Table A.3 shows the number of particles released per month and site.

Table A.1
Mouth rivers location, weighting factor w_j for each river and the factor f from González-Fernández et al. (2021).

	Aguera	Ulla	Guadalquivir
Latitude	43.41	42.64	36.78
Longitude	−3.31	−8.76	−6.44
Factor w_j	1.00	4.73	13.62
f	26.824	126.995	367.913

Table A.2
Monthly mean river flows and number of particles released per month and river, Eq. A.2.

	Monthly mean river flow (m^3/s)			Particles released		
	Aguera	Ulla	Guadalquivir	Aguera	Ulla	Guadalquivir
Jan 17	0,98	2,75	10,09	34	450	4785
Feb 17	0,84	3,21	11,38	29	524	5393
Mar 17	0,82	2,99	29,62	28	489	14.041
Apr 17	0,74	2,88	36,86	25	471	17.475
May 17	0,68	2,88	35,61	24	471	16.881
Jun 17	0,65	2,73	26,45	22	447	12.539
Jul 17	0,60	2,54	9,80	21	416	4644
Aug 17	0,58	2,47	8,65	20	404	4100
Sep 17	0,77	2,46	8,26	27	402	3914
Oct 17	0,64	2,55	6,01	22	417	2847
Nov 17	0,88	2,65	7,07	31	434	3350
Dec 17	1,27	2,83	9,09	44	464	4311
TOTAL	9,45	32,95	198,88	327	5391	94.282

Table A.3
Relative importance of emissions from the on-land sites considered in the simulation and number of particles released per month and site. These values have been estimated according to MAPAMA (Ministerio de Agricultura y Pesca and Públicas) (2012a,b).

Source name	Lat	Lon	Intensity	Particles released
Palmas S	27.82	−15.41	4*1	4*144
Tenerife SE	28.01	−16.60		
Tenerife SW	28.03	−16.72		
Tenerife NW	28.58	−16.25		
Lanzarote	29.00	−13.46	3*2	3*288
Tenerife NE_1	28.37	−16.33		
Tenerife NE_2	28.44	−16.22		
Puerto Palmas	28.11	−15.40	2*3	2*431
Puerto Palmas 2	28.14	−15.47		
Bilbao	43.36	−3.04	4*4	4*575
Gijón	43.59	−5.73		

(continued on next page)

Table A.3 (*continued*)

Source name	Lat	Lon	Intensity	Particles released
Avilés	43.59	−5.96		
Arousa	42.50	−8.95		
Santander	43.48	−3.75	4*5	4*718
Coruña	43.42	−8.37		
Vigo	42.19	−8.85		
Huelva	37.18	−7.03		
Cádiz	36.56	−6.33	6	862

Data availability

Data will be made available on request.

References

Alberola, C., Millot, C., Font, J., 1995. On the seasonal and mesoscale variabilities of the northern current during the PRIMO-0 experiment in the western Mediterranean Sea. Oceanol. Acta 18, 163–192.

Alfaro-Núñez, A., Astorga, D., Cáceres-Farías, L., Bastidas, L., Soto Villegas, C., Macay, K., Christensen, J.H., 2021. Microplastic pollution in seawater and marine organisms across the tropical eastern Pacific and Galápagos. Sci. Rep. 11, 6424. https://doi.org/10.1038/s41598-021-85939-3.

Amelia, T.S.M., Khalik, W.M.A.W.M., Ong, M.C., Shao, Y.T., Pan, H.J., Bhubalan, K., 2021. Marine microplastics as vectors of major ocean pollutants and its hazards to the marine ecosystem and humans. Prog Earth Planet Sci 8, 1–26.

André, G., Garreau, P., Garnier, V., Fraunié, P., 2005. Modelled variability of the sea surface circulation in the North-Western Mediterranean Sea and in the Gulf of lions. Ocean Dyn. 55, 294–308. https://doi.org/10.1007/s10236-005-0013-6.

Basurko, O.C., Ruiz, I., Rubio, A., Beldarrain, B., Kukul, D., Cózar, A., Galli, M., Destang, T., Larreta, J., 2022. The coastal waters of the south-east bay of Biscay a dead-end for neustonic plastics. Mar. Pollut. Bull. 181, 113881. https://doi.org/10.1016/j.marpolbul.2022.113881.

Bauer-Civiello, A., Critchell, K., Hoogenboom, M., Hamann, M., 2019. Input of plastic debris in an urban tropical river system. Mar. Pollut. Bull. 144, 235–242. https://doi.org/10.1016/j.marpolbul.2019.04.070.

Baztan, J., Carrasco, A., Chouinard, O., Cleaud, M., Gabaldon, J.E., Huck, T., Jaffrès, L., Jorgensen, B., Miguelez, A., Paillard, C., Vanderlinden, J.P., 2014. Protected areas in the Atlantic facing the hazards of micro-plastic pollution: first diagnosis of three islands in the canary current. Mar. Pollut. Bull. 80, 302–311. https://doi.org/10.1016/j.marpolbul.2013.12.052.

Bhagat, J., Zang, L., Nishimura, N., Shimada, Y., 2020. Zebrafish: an emerging model to study microplastic and nanoplastic toxicity. Sci. Total Environ. 728, 138707.

van Calcar, C.v., van Emmerik, T.v., 2019. Abundance of plastic debris across european and asian rivers. Environ. Res. Lett. 14, 124051.

Campuzano, F., Brito, D., Juliano, M., Fernandes, R., de Pablo, H., Neves, R., 2016. Coupling watersheds, estuaries and regional ocean through numerical modelling for western Iberia: a novel methodology. Ocean Dynamics 66, 1745–1756.

Carlson, D.F., Suaria, G., Aliani, S., Fredj, E., Fortibuoni, T., Griffa, A., Russo, A., Melli, V., 2017. Combining litter observations with a regional ocean model to identify sources and sinks of floating debris in a semi-enclosed basin: the adriatic sea. Front. Mar. Sci. 4, 78.

Charria, G., Lazure, P., Le Cann, B., Serpette, A., Reverdin, G., Louazel, S., Batifoulier, F., Dumas, F., Pichon, A., Morel, Y., 2013. Surface layer circulation derived from lagrangian drifters in the bay of Biscay. J. Mar. Syst. 109, S60–S76.

Chassignet, E.P., Xu, X., Zavala-Romero, O., 2021. Tracking marine litter with a global ocean model: where does it go? Where does it come from? Front. Mar. Sci. 8, 667591.

Cividanes, M., Aguiar-González, B., Gómez, M., Herrera, A., Martínez, I., Pham, C.K., Pérez, L., Machín, F., 2024. Lagrangian tracking of long-lasting plastic tags: from lobster fisheries in the Usa and Canada to macaronesia. Mar. Pollut. Bull. 198, 115908. https://doi.org/10.1016/j.marpolbul.2023.115908.

Cloux, S., Allen-Perkins, S., de Pablo, H., Garaboa-Paz, D., Montero, P., Pérez-Muñuzuria, V., 2022. Validation of a Lagrangian model for large-scale macroplastic tracer transport using mussel-peg in NW Spain (Ría de Arousa). Sci. Total Environ. 822, 153338. https://doi.org/10.1016/j.scitotenv.2022.153338.

Copernicus, n.d.,. Copernicus marine service. URL: https://data.marine.copernicus.eu/product/GLOBAL_ANALYSIS_FORECAST_PHY_001_024/description.

Cozar, A., Echevarria, F., Gonzalez-Gordillo, J.I., Irigoien, X., Ubeda, B., Hernandez-Leon, S., Palma, A.T., Navarro, S., Garcia-de Lomas, J., Ruiz, A., Fernandez-de Puelles, M.L., Duarte, C.M., 2014. Plastic debris in the open ocean. Proc. Natl. Acad. Sci. 111, 10239–10244. https://doi.org/10.1073/pnas.1314705111.

Criado-Aldeanueva, F., García-Lafuente, J., Navarro, G., Ruiz, J., 2009. Seasonal and interannual variability of the surface circulation in the eastern gulf of cadiz (sw Iberia). J. Geophys. Res. Oceans 114.

Critchell, K., Lambrechts, J., 2016. Modelling accumulation of marine plastics in the coastal zone; what are the dominant physical processes? Estuar. Coast. Shelf Sci. 171, 111–122. https://doi.org/10.1016/j.ecss.2016.01.036.

Dagestad, K.F., Röhrs, J., Breivik, Ø., Ådlandsvik, B., 2018. Opendrift v1. 0: a generic framework for trajectory modelling. Geosci. Model Dev. 11, 1405–1420.

Declerck, A., Delpey, M., Rubio, A., Ferrer, L., Basurko, O., Mader, J., Louzao, M., 2019. Transport of floating marine litter in the coastal area of the south-eastern bay of Biscay: a lagrangian approach using modelling and observations. Journal of Operational Oceanography 12, S111–S125.

Dietrich, G., Kalle, K., 1957. General Oceanography; an Introduction. Interscience Pub, New York (USA).

van Duinen, B., Kaandorp, M.L., Van Sebille, E., 2022. Identifying marine sources of beached plastics through a bayesian framework: application to Southwest Netherlands. Geophys. Res. Lett. 49, e2021GL097214.

Duncan, E.M., Botterell, Z.L., Broderick, A.C., Galloway, T.S., Lindeque, P.K., Nuno, A., Godley, B.J., 2017. A global review of marine turtle entanglement in anthropogenic debris: A baseline for further action. https://doi.org/10.3354/esr00865.

Eriksen, M., Lebreton, L.C., Carson, H.S., Thiel, M., Moore, C.J., Borerro, J.C., Galgani, F., Ryan, P.G., Reisser, J., 2014. Plastic pollution in the world's oceans: more than 5 trillion plastic pieces weighing over 250,000 tons afloat at sea. PloS One 9, e111913.

Flexas, M.d.M., Gomis, D., Ruiz, S., Pascual, A., León, P., 2006. In situ and satellite observations of the eastward migration of the western alboran sea gyre. Prog. Oceanogr. 70, 486–509.

Friocourt, Y., Levier, B., Speich, S., Blanke, B., Drijfhout, S., 2007. A regional numerical ocean model of the circulation in the bay of Biscay. J. Geophys. Res. Oceans 112.

González-Fernández, D., Cózar, A., Hanke, G., Viejo, J., Morales-Caselles, C., Bakiu, R., Barceló, D., Bessa, F., Bruge, A., Cabrera, M., Castro-Jiménez, J., Constant, M., Crosti, R., Galletti, Y., Kideys, A.E., Machitadze, N., Pereira de Brito, J., Pogojeva, M., Ratola, N., Rigueira, J., Rojo-Nieto, E., Savenko, O., Schöneich-Argent, R.I., Siedlewicz, G., Suaria, G., Tourgeli, M., 2021. Floating macrolitter leaked from Europe into the ocean. Nature Sustainability 4, 474–483. https://doi.org/10.1038/s41893-021-00722-6.

Haynes, R., Barton, E.D., 1990. A poleward flow along the Atlantic coast of the Iberian peninsula. J. Geophys. Res. Oceans 95 (C7), 11425–11441. https://doi.org/10.1029/JC095iC07p11425.

Hernández-Sánchez, C., González-Sálamo, J., Díaz-Peña, F.J., Fraile-Nuez, E., Hernández-Borges, J., 2021. Arenas Blancas (el hierro island), a new hotspot of plastic debris in the canary islands (Spain). Mar. Pollut. Bull. 169, 112548. https://doi.org/10.1016/j.marpolbul.2021.112548.

Herrera, A., Acosta-Dacal, A., Luzardo, O.P., Martínez, I., Rapp, J., Reinold, S., Montesdeoca-Esponda, S., Montero, D., Gómez, M., 2022. Bioaccumulation of additives and chemical contaminants from environmental microplastics in european seabass (dicentrarchus labrax). Sci. Total Environ. 822, 153396.

Hwang, J., Choi, D., Han, S., Jung, S.Y., Choi, J., Hong, J., 2020. Potential toxicity of polystyrene microplastic particles. Sci. Rep. 10, 7391.

Iskandar, M.R., Surinati, D., Cordova, M.R., Siong, K., 2021. Pathways of floating marine debris in Jakarta bay, Indonesia. Mar. Pollut. Bull. 169, 112511.

Jalón-Rojas, I., Wang, X.H., Fredj, E., 2019a. A 3d numerical model to track marine plastic debris (trackmpd): sensitivity of microplastic trajectories and fates to particle dynamical properties and physical processes. Mar. Pollut. Bull. 141, 256–272. https://doi.org/10.1016/j.marpolbul.2019.02.052.

Jalón-Rojas, I., Wang, X.H., Fredj, E., 2019b. A 3d numerical model to track marine plastic debris (trackmpd): sensitivity of microplastic trajectories and fates to particle dynamical properties and physical processes. Mar. Pollut. Bull. 141, 256–272.

Jambeck, J.R., Geyer, R., Wilcox, C., Siegler, T.R., Perryman, M., Andrady, A., Narayan, R., Law, K.L., 2015. Plastic waste inputs from land into the ocean. Science 347, 768–771. https://doi.org/10.1126/science.1260352.

Karbalaei, S., Hanachi, P., Walker, T.R., Cole, M., 2018. Occurrence, sources, human health impacts and mitigation of microplastic pollution. Environ. Sci. Pollut. Res. 25, 36046–36063. https://doi.org/10.1007/s11356-018-3508-7.

Khoirunnisa, H., Wibowo, M., Hendriyono, W., 2020. Determination of Construction Design to Reduce the Amount of Marine Litter at Seawater Intake Using Particle Tracking Module of Numerical Method by Mike 21 (Case Study: Tanjung Awar – Awar). Tuban, East Java. https://doi.org/10.1088/1742-6596/1625/1/012045.

Krause, S., Molari, M., Gorb, E.V., Gorb, S.N., Kossel, E., Haeckel, M., 2020. Persistence of plastic debris and its colonization by bacterial communities after two decades on the abyssal seafloor. Sci. Rep. https://doi.org/10.1038/s41598-020-66361-7.

Krauss, W., 1986. The North Atlantic current. J. Geophys. Res. 91, 5061. https://doi.org/10.1029/jc091ic04p05061.

Lange, M., van Sebille, E., 2017. Parcels v0. 9: prototyping a lagrangian ocean analysis framework for the petascale age. Geosci. Model Dev. 10, 4175–4186.

Lavender, S., 2022. Detection of waste plastics in the environment: application of copernicus earth observation data. Remote Sens. (Basel) 14. https://doi.org/10.3390/rs14194772.

Lebreton, L.C., Van Der Zwet, J., Damsteeg, J.W., Slat, B., Andrady, A., Reisser, J., 2017. River plastic emissions to the world's oceans. Nat. Commun. 8, 15611.
Lebreton, L.M., Greer, S., Borrero, J., 2012. Numerical modelling of floating debris in the world's oceans. Mar. Pollut. Bull. 64, 653–661. https://doi.org/10.1016/j.marpolbul.2011.10.027.
Liu, B., Hou, L., Wang, Y., Ma, W., Yan, B., Li, X., Chen, G., 2020. Emission estimate and countermeasures of marine plastic debris and microplastics in China. Res. Environ. Sci. https://doi.org/10.13198/j.issn.1001-6929.2019.07.05.
Mann, C.R., 1967. The termination of the Gulf stream and the beginning of the North Atlantic current. Deep-Sea Res. Oceanogr. Abstr. 337–359.
Mann, C.R., 1972. A review of the branching of the Gulf stream system. Proceedings of the Royal Society of Edinburgh, Section B: Biological Sciences 72, 341–349.
MAPAMA (Ministerio de Agricultura y Pesca, A.y.M.A., Públicas), C.C.d.E.y.E.d.O., 2012a. Acumulación de presiones que pueden causar la entrada de basuras al mar desde tierra en la Demarcación Noratlántica (EM NOR PRE Basura Terrestre). URL: http://infomar.cedex.es:8080/geonetwork/srv/spa/catalog.search;jsessionid=node01ozdfxabk663h1tw377hxbz5hp5184.node0#/metadata/03d74c07-d5a0-4242-8217-95463efff062.
MAPAMA (Ministerio de Agricultura y Pesca, A.y.M.A., Públicas), C.C.d.E.y.E.d.O., 2012b. Acumulación de presiones que pueden provocar la entrada de basuras en el mar desde tierra en la Demarcación Sudatlántica (EM SUD PRE Basura Terrestre). URL: http://infomar.cedex.es:8080/geonetwork/srv/spa/catalog.search;jsessionid=node01ozdfxabk663h1tw377hxbz5hp5184.node0#/metadata/88f254fb-67ea-49a7-9138-e7eeaeb9050f.
Martínez, J., García-Ladona, E., Joaquim Ballabrera-Poy, J.I.F., González-Motos, S., Allegue, J.M., González-Haro, C., 2022. Atlas of surface currents in the mediterranean and canary–iberian–Biscay waters. Journal of Operational Oceanography 0, 1–23. https://doi.org/10.1080/1755876X.2022.2102357.
Masiá, P., Ardura, A., Gaitán, M., Gerber, S., Rayon-Viña, F., Garcia-Vazquez, E., 2021. Maritime ports and beach management as sources of coastal macro-, meso-, and microplastic pollution. Environ. Sci. Pollut. Res. 28, 30722–30731.
Maxey, M.R., Riley, J.J., 1983. Equation of motion for a small rigid sphere in a nonuniform flow. The Physics of Fluids 26, 883–889. https://doi.org/10.1063/1.864230.
Mecho, A., Francescangeli, M., Ercilla, G., Fanelli, E., Estrada, F., Valencia, J., Sobrino, I., Danovaro, R., Company, J.B., Aguzzi, J., 2020. Deep-sea litter in the gulf of cadiz (northeastern Atlantic, Spain). Mar. Pollut. Bull. 153, 110969. https://doi.org/10.1016/j.marpolbul.2020.110969.
Millot, C., 1999. Circulation in the western mediterranean sea. J. Mar. Syst. 20, 423–442.
Min, K., Cuiffi, J.D., Mathers, R.T., 2020. Ranking environmental degradation trends of plastic marine debris based on physical properties and molecular structure. Nat. Commun. 11, 727.
Onink, V., Jongedijk, C.E., Hoffman, M.J., van Sebille, E., Laufkötter, C., 2021. Global simulations of marine plastic transport show plastic trapping in coastal zones. Environ. Res. Lett. 16, 064053.
de Pablo, H., Sobrinho, J., Garaboa-Paz, D., Fonteles, C., Neves, R., Gaspar, M.B., 2022. The influence of the river discharge on residence time, exposure time and integrated water fractions for the Tagus estuary (Portugal). Front. Mar. Sci. 8, 1–16. https://doi.org/10.3389/fmars.2021.734814.
Peliz, A., Dubert, J., Marchesiello, P., Teles-Machado, A., 2007. Surface circulation in the gulf of cadiz: model and mean flow structure. J. Geophys. Res. Oceans 112. https://doi.org/10.1029/2007JC004159.
Peliz, A., Boutov, D., Teles-Machado, A., 2013. The alboran sea mesoscale in a long term high resolution simulation: statistical analysis. Ocean Model. 72, 32–52.
Pereiro, D., Souto, C., Gago, J., 2018. Calibration of a marine floating litter transport model. J. Oper. Oceanogr. 11, 125–133. https://doi.org/10.1080/1755876X.2018.1470892.
Pereiro, D., Souto, C., Gago, J., 2019. Dynamics of floating marine debris in the northern iberian waters: a model approach. J. Sea Res. 144, 57–66.
Perkins, H., Kinder, T., La Violette, P., 1990. The Atlantic inflow in the western alboran sea. J. Phys. Oceanogr. 20, 242–263.
Politikos, D.V., Tsiaras, K., Papatheodorou, G., Anastasopoulou, A., 2020. Modeling of floating marine litter originated from the eastern Ionian Sea: transport, residence time and connectivity. Mar. Pollut. Bull. https://doi.org/10.1016/j.marpolbul.2019.110727.
Rangel-Buitrago, N., Williams, A., Costa, M.F., de Jonge, V., 2020. Curbing the inexorable rising in marine litter: an overview. Ocean & Coastal Management 188, 105133.
Ruiz, I., Ana .A., J., Basurko, O.C., Rubio, A., 2022. Modelling the distribution of fishing-related floating marine litter within the bay of Biscay and its marine protected areas. Environ. Pollut. 292, 118216. https://doi.org/10.1016/j.envpol.2021.118216.
Ryan, P.G., 2018. Entanglement of birds in plastics and other synthetic materials. Mar. Pollut. Bull. 135, 159–164. https://doi.org/10.1016/j.marpolbul.2018.06.057.
Sobrinho, J., Canelas, R., Garaboa-Paz, A., Campuzano, F., 2023. Mohid-Lagrangian GitHub. URL. https://github.com/Mohid-Water-Modelling-System/MOHID-Lagrangian.
Solabarrieta, L., Rubio, A., Castanedo, S., Medina, R., Charria, G., Hernandez, C., 2014. Surface water circulation patterns in the southeastern bay of Biscay: new evidences from hf radar data. Cont. Shelf Res. 74, 60–76.
Sousa, M.C., deCastro, M., Gago, J., Ribeiro, A.S., Des, M., Gómez-Gesteira, J.L., Dias, J. M., Gomez-Gesteira, M., 2021. Modelling the distribution of microplastics released by wastewater treatment plants in ria de Vigo (nw iberian peninsula). Mar. Pollut. Bull. 166, 112227. https://doi.org/10.1016/j.marpolbul.2021.112227.
Stuparu, D., van der Meulen, M., Kleissen, F., Vethaak, D., El Serafy, G., 2015. Developing a transport model for plastic distribution in the North Sea. volume 28.
Sutherland, B.R., DiBenedetto, M., Kaminski, A., van den Bremer, T., 2023. Fluid dynamics challenges in predicting plastic pollution transport in the ocean: a perspective. Phys. Rev. Fluids 8, 070701. https://doi.org/10.1103/PhysRevFluids.8.070701.
Talley, L.D., 2011. Descriptive Physical Oceanography: An Introduction. Academic press.
Tsiaras, K., Hatzonikolakis, Y., Kalaroni, S., Pollani, A., Triantafyllou, G., 2021. Modeling the pathways and accumulation patterns of micro-and macro-plastics in the mediterranean. Front. Mar. Sci. 8, 743117.
Tulloch, V., Pirotta, V., Grech, A., Crocetti, S., Double, M., How, J., Kemper, C., Meager, J., Peddemors, V., Waples, K., Watson, M., Harcourt, R., 2020. Long-term trends and a risk analysis of cetacean entanglements and bycatch in fisheries gear in Australian waters. Biodivers. Conserv. 29, 251–282. https://doi.org/10.1007/s10531-019-01881-x.
Turrell, W., 2020. How litter moves along a macro tidal mid-latitude coast exposed to a coastal current. Mar. Pollut. Bull. 160, 111600.
Van Aken, H.M., 2001. The hydrography of the mid-latitude Northeast Atlantic Ocean—part iii: the subducted thermocline water mass. Deep-Sea Res. I Oceanogr. Res. Pap. 48, 237–267.
Van Emmerik, T., Kieu-Le, T.C., Loozen, M., Van Oeveren, K., Strady, E., Bui, X.T., Egger, M., Gasperi, J., Lebreton, L., Nguyen, P.D., et al., 2018. A methodology to characterize riverine macroplastic emission into the ocean. Front. Mar. Sci. 5, 372.
Van Sebille, E., Wilcox, C., Lebreton, L., Maximenko, N., Hardesty, B.D., Van Franeker, J. A., Eriksen, M., Siegel, D., Galgani, F., Law, K.L., 2015. A global inventory of small floating plastic debris. Environ. Res. Lett. 10, 124006. https://doi.org/10.1088/1748-9326/10/12/124006.
Van Sebille, E., Aliani, S., Law, K.L., Maximenko, N., Alsina, J.M., Bagaev, A., Bergmann, M., Chapron, B., Chubarenko, I., Cózar, A., et al., 2020. The physical oceanography of the transport of floating marine debris. Environ. Res. Lett. 15, 023003.
Vargas-Yáñez, M., Plaza, F., Garcıa-Lafuente, J., Sarhan, T., Vargas, J., Vélez-Belchí, P., 2002. About the seasonal variability of the alboran sea circulation. J. Mar. Syst. 35, 229–248.
Vélez-Belchí, P., Pérez-Hernández, M., Casanova-Masjoan, M., Cana, L., Hernández-Guerra, A., 2017. On the seasonal catiability of the canary current and the Atlantic meridional overturning circulation. J. Geophys. Res. Oceans 122, 4518–4538. https://doi.org/10.1038/175238c0.
Wayman, C., Niemann, H., 2021. The fate of plastic in the ocean environment-a minireview. Environ. Sci.: Processes Impacts 23, 198–212. https://doi.org/10.1039/d0em00446d.
Williams, A., Rangel-Buitrago, N., 2019. Marine litter: solutions for a major environmental problem. J. Coast. Res. 35, 648. https://doi.org/10.2112/JCOASTRES-D-18-00096.1.
Zambianchi, E., Trani, M., Falco, P., 2017. Lagrangian transport of marine litter in the mediterranean sea. Front. Environ. Sci. 5, 5. https://doi.org/10.3389/fenvs.2017.00005.